Quantum Localization in Rough Billiards

Klaus M. Frahm and Dima L. Shepelyansky*
Laboratoire de Physique Quantique, UMR C5626 du CNRS, Université Paul Sabatier, F-31062 Toulouse Cedex 4, France
(Received 2 December 1996)

We study the level spacing statistics $p(s)$ and eigenfunction properties in a billiard with a rough boundary. Quantum effects lead to localization of classical diffusion in the angular momentum space and the Shnirelman peak in $p(s)$ at small s. The ergodic regime with Wigner-Dyson statistics is identified as a function of roughness. Applications to Q spoiling in optical resonators are also discussed. [S0031-9007(97)02470-8]

PACS numbers: 05.45.+b, 72.15.Rn, 03.65.Sq

In 1984, Bohigas, Giannoni, and Schmit [1] demonstrated that random matrix theory (RMT) [2] describes the level spacing statistics of classically chaotic billiards. After that such types of billiards have been studied in great detail by different groups [3]. However, all the billiards under investigation were characterized only by one typical time scale τ_c, namely, the time between collisions with the boundary. Another type of chaotic systems with diffusive behavior, like the kicked rotator [4], has an additional much longer time scale $\tau_D \gg \tau_c$ which is required to cover the accessible phase space. In this situation quantum interference effects may lead to exponential localization of the eigenstates and disappearance of level repulsion.

Recently, it has been shown [5] that the diffusive regime also appears in a nearly circular Bunimovich stadium billiard. The authors of [5] gave an estimate for the localization length in the angular momentum space and found the energy border $E_{\rm erg}$ above which the eigenstates become ergodic on the energy surface [6]. Their numerical results demonstrate the change of level statistics from Wigner-Dyson to Poisson when the energy becomes smaller than $E_{\rm erg}$. However, this example, while very interesting for mathematical studies, is not realistic for physical systems.

At the same time a great progress has been reached in optics of microcavities like micrometer-size droplets [7] and microdisk lasers [8]. The industrial request to produce directed light pushed the researchers to investigate ray dynamics in weakly deformed circular billiards and droplets. It was shown that above some critical deformation the ray dynamics becomes chaotic. As a consequence the directionality of light from droplets and Q factors of such resonators are strongly affected [9]. However, due to the smoothness of deformation the diffusive regime was hardly accessible in such systems.

In this Letter, we investigate another type of generic boundary deformation which may have important physical applications. Namely, we consider billiards with a rough boundary. In this approach, the boundary is a random surface with some finite correlation length. The physical realizations of such a situation can be quite different. As examples, we can mention surface waves in the droplets which are practically static for the light [7], nonideal surfaces in microdisk lasers [8], and capillary waves on a surface of small metallic clusters [10]. On a first glance it seems that such a rough boundary in a circular billiard will destroy the conservation of angular momentum l leading to ergodic eigenstates and RMT level statistics. In spite of this we show that there is a region of roughness in which the classical dynamics is chaotic but the eigenstates are localized and the level spacing statistics $p(s)$ has the sharp Shnirelman peak at small spacings s [11,12]. We also demonstrate the close relation between this model and the kicked rotator.

As a model of a rough billiard we chose a circle with a deformed elastic boundary given by $R(\theta) = R_0 + \Delta R(\theta)$ with $\Delta R(\theta)/R_0 = \text{Re} \sum_{m=2}^{M} \gamma_m e^{im\theta}$. Here γ_m are random complex coefficients and M is large but finite. The surface roughness is given by $\kappa(\theta) = (dR/d\theta)/R_0$. In the following, we will consider the case of weak roughness $\kappa \ll 1$. One can model different types of surfaces by choosing an appropriate dependence of amplitudes on m. However, our results show that in the domain of strong chaos the classical diffusion and quantum localization in orbital momentum space are determined by the angle average $\tilde{\kappa}^2 = \langle \kappa^2(\theta) \rangle_\theta$. Because of that we choose a typical dependence $\gamma_m \sim 1/m$ such that all harmonics give the same contribution in $\tilde{\kappa}^2 \sim M(\Delta R/R_0)^2$.

First, we consider the classical ray dynamics which for $\kappa \ll 1$ can be described by the following *rough* map:

$$\bar{l} = l + 2\sqrt{l_{\max}^2 - l_r^2}\,\kappa(\theta)\,,$$
$$\bar{\theta} = \theta + \pi - 2\arcsin(\bar{l}/l_{\max})\,. \qquad (1)$$

Here the first equation gives the change of l (and velocity vector) due to the collision with boundary and the second one the change of angle between collisions. This map describes the dynamics in the vicinity of a resonant value l_r defined by the condition $\bar{\theta} = \theta + 2\pi r$ with integer r, and $l_{\max}$ is the maximal l at given particle velocity v. Our numerical simulations of exact ray dynamics show that the rough map (1) indeed gives an excellent description (see Fig. 1). A similar map for a stadium billiard was given in [5]. However, in contrast to [5], where $\kappa(\theta)$ has a discontinuity, the global chaos sets in

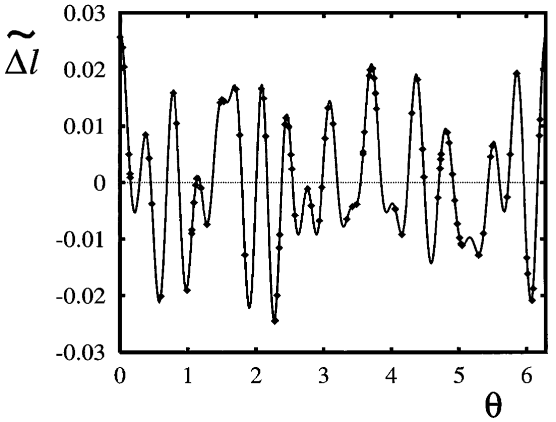

FIG. 1. Comparison of the exact dynamics (points) and the rough map (1) [full curve $\kappa(\theta)$]. The points correspond to $\tilde{\Delta l} = (\bar{l} - l)/(2\sqrt{l_{\max}^2 - l^2})$ and $M = 20$, $\tilde{\kappa} = 0.011$.

only if the roughness is above some critical value $\tilde{\kappa} > \kappa_c$. Below κ_c the KAM theory is valid and the phase space is divided by invariant curves. The chaos border can be estimated on the basis of Chirikov criteria of overlapping resonances [13] which gives $\kappa_c \sim 4M^{-5/2}$ (the numerical coefficient is extracted from the data for $M = 20$). This border drops strongly with M, and therefore we will concentrate on the regime of strong chaos without visible islands of stability (case of Fig. 1). In this regime the spreading in angular momentum space goes in a diffusive way with a diffusion constant that is easily estimated from (1) as $D = (\Delta l)^2/\Delta t = 4(l_{\max}^2 - l_r^2)\tilde{\kappa}^2$ where Δt is measured in number of collisions. The physical time required for diffusive spreading over the energy surface is $\tau_D \approx \tau_c l_{\max}^2/D$ with $\tau_c \sim R_0/v$.

Now, we turn to the investigation of the quantum problem. For this we expand the wave function $\psi(r,\theta)$ with energy $E = \hbar^2k^2/2m$ in terms of the Hankel functions which form a complete set,

$$\psi(r,\theta) = \sum_l [a_l H_{|l|}^{(+)}(kr)e^{il\theta} + b_l H_{|l|}^{(-)}(kr)e^{il\theta}]. \quad (2)$$

The regularity of ψ at $r = 0$ requires $a_l = b_l$ so that a_l are the amplitudes in angular momentum space. The boundary condition $\psi[R(\theta),\theta] = 0$ results in a second equation $b_l = \sum_{l'} S_{ll'}(E)a_{l'}$ where $S_{ll'}(E)$ has the meaning of a scattering matrix for waves reflected at the rough boundary. The energy eigenvalues are determined by $\det[1 - S(E)] = 0$. A convenient expression for the S matrix can be obtained by the quasiclassical approximation $H_l^{(\pm)}(kr) \approx 2[2\pi k_l(r)r]^{-1/2}\exp\{\pm i\mu_l(r) - \pi/4]\}$ where $k_l(r) = k(1 - r_l^2/r^2)^{1/2}$, $\mu_l(r) = \int_{r_l}^r d\tilde{r}\, k_l(\tilde{r})$, and $r_l \approx |l|/k$ is the classical turning point. From this representation and the boundary condition for ψ we obtain (for more details see [14])

$$S_{ll'} \approx e^{i\mu_l(R_0)+i\mu_{l'}(R_0)+i\pi/2}\langle l|e^{i\,2k_{l_r}(R_0)\,\Delta R(\theta)}|l'\rangle. \quad (3)$$

This is a local unitary expression for S near l_r which is valid for $\Delta l = |l - l'| \ll l_{\max} = kR_0$ and $M < l_{\max}$. A stationary phase approximation for the θ integral gives the classical change of l [see (1)] and determines the structure of S matrix. In fact, this matrix is very similar to the evolution operator of the kicked rotator [4] corresponding to $\Delta R \propto \cos\theta$. According to this analogy the localization length ℓ is determined by the classical diffusion rate $\ell = \beta D/2$ where β is the symmetry index for orthogonal ($\beta = 1$) [15] or local unitary symmetry ($\beta = 2$) [16]. Since generally $\Delta R(\theta) \neq \Delta R(-\theta)$, we have $\beta = 2$ so that the localization length is directly determined by the roughness

$$\ell = D = 4(l_{\max}^2 - l_r^2)\tilde{\kappa}^2. \quad (4)$$

This result can also be derived on a more rigorous ground based on the supersymmetry approach for a model with random phases μ_l [14]. The expression (4) is only valid for $D > M$ while $1 < D < M$ corresponds to a more complicated regime with $\ell \sim M$ (see below). For $1 < D \ll l_{\max}$ the eigenfunctions are exponentially localized in the orbital space $|a_l| \propto \exp(-|l - l_0|/\ell)$ while the classical dynamics is ergodic on the whole energy surface. The quantum dynamics becomes ergodic only for $\ell > l_{\max}$. According to the Weyl formula the level number at energy E is $N \approx mR_0^2E/2\hbar^2 = l_{\max}^2/4$. Therefore the states are ergodic for

$$N > N_e \approx \frac{1}{64\tilde{\kappa}^4}. \quad (5)$$

This border is much higher than the perturbative border $N < N_p \approx 1/(16\tilde{\kappa}^2)$ where the diffusion mixes less than one state ($D \approx 1$). These different regimes are presented in Fig. 2.

To check the above theoretical predictions, we have solved numerically the boundary condition for $\psi(r,\theta)$ (2).

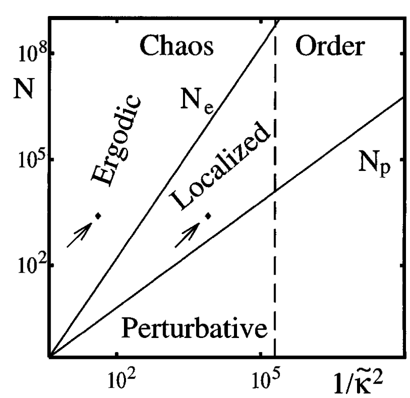

FIG. 2. Global diagram showing the eigenstate properties for different values of level number N and roughness $\tilde{\kappa}$ for $D \gg M$. The two full lines give the ergodic (N_e) and perturbative (N_p) borders, the dashed line is the classical chaos border $\kappa_c \approx 0.002$ for $M = 20$. The parameters of Figs. 3 and 4 are shown by the two points with arrows.

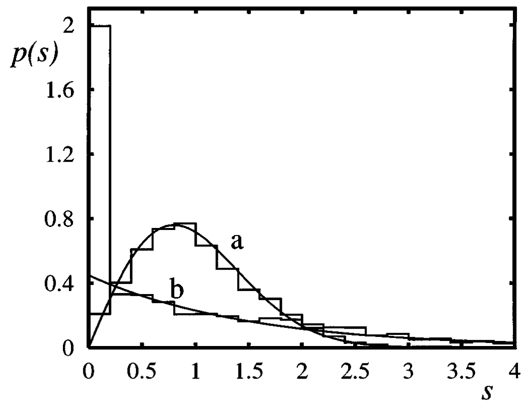

FIG. 3. Level spacing distribution $p(s)$ for $l_{\max} \approx 100$, $M = 20$, and average roughness: (a) $\tilde{\kappa} \approx 0.16$ (ergodic, $\ell \approx 1000$) and (b) $\tilde{\kappa} \approx 0.012$ (localized, $\ell \approx 6$). The total statistics is 2000 levels ($2150 < N < 2350$) from ten different realizations of the rough boundary. Also shown are the Wigner-Dyson and rescaled Poisson distributions with $\alpha = 0.33$.

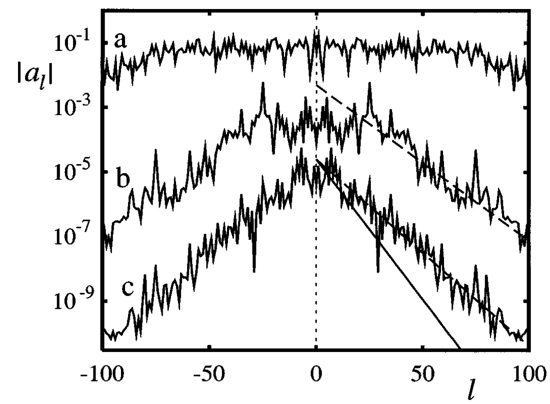

FIG. 4. The amplitudes $|a_l|$ for three typical eigenfunctions corresponding to the parameters of Fig. 3 (with level number $N \sim 2250$): (a) ergodic case; (b) localized quasidegenerate state with $s = 0.1$ and fitted localization length $\ell \approx 9$ (dashed line); (c) nondegenerate localized state with fitted $\ell \approx 7.5$ (dashed line). The full line shows the theoretical length [see Eq. (4)] $\ell \approx 5$. The rough boundary realization is the same as in Figs. 1(b) and 1(c) or appropriately rescaled (a). The curves b and c are shifted by factors 10^{-2} or 10^{-4}, respectively.

In this way, we have obtained both the energy eigenvalues and the amplitudes a_l (with normalization $\sum_l |a_l|^2 = 1$). In the ergodic regime $N > N_e$, we find that the level spacing statistics $p(s)$ is in a good agreement with RMT (see Fig. 3). On the contrary, in the localized regime $N < N_e$, approximately each second level is quasidegenerate leading to the Shnirelman peak [11] at small spacings (Fig. 3). This peak represents approximately a fraction $\alpha \approx 0.33$ of all spacings. The other spacings are described by a rescaled Poisson distribution $p(s) = (1 - \alpha)^2 \exp[-(1 - \alpha)s]$. The appearance of the Shnirelman peak is in agreement with the prediction made in [12]. Its physical origin is the time reversal symmetry ($S^{\dagger}_{-l,-l'} = S^{*}_{ll'}$ or $a_{-l} = a_l^*$) due to which two states localized around l_0 and $-l_0$ form a quasidegenerate pair of symmetric and antisymmetric states [17]. The original Shnirelman theorem was formulated for quasi-integrable billiards [11]. Our case corresponds to the chaotic domain; however, because of localization the peak still exists. A similar situation for the kicked rotator was studied in [12]. The fraction of nondegenerate levels ($1 - 2\alpha \approx 0.34$) is due to states localized near $l_0 \approx 0$. The measure of such states is approximately $4\ell/l_{\max} \approx 1 - 2\alpha$ where the numerical coefficient was extracted from our data (see Fig. 4). This peak was not found in [5] because the stadium billiard has additional symmetries and only the states of one parity were considered.

In Fig. 4, we show three typical eigenfunctions in angular momentum representation. In the ergodic case, the probability is homogeneously distributed, almost in the whole interval $(-l_{\max}, l_{\max})$. We mention that in our computations we have included about ten evanescent modes (with $|l| > kR_0$). The two other wave functions are in the localized regime of Fig. 2 with $\ell \ll l_{\max}$. One of them has a double peak structure due to tunneling between time reversed angular momentum states. This state corresponds to a quasidegenerate Shnirelman state. We also observed many other similar states with much smaller level splitting ($s < 10^{-2}$). The other localized state has the maximum $l_0 \approx 0$ and corresponds to a nondegenerate level. Both states clearly show exponential localization indicated by the dashed lines. The numerical values of the localization length are a bit higher than the estimate (4) with $l_r \approx l_0 \ll l_{\max}$.

To understand this discrepancy, we have calculated ℓ for a wide region of M and $\tilde{\kappa}$. Many cases were systematically different from (4). To increase the parameter range we also studied the effective kicked rotator model with random phases μ_l in the evolution operator (3) (and $l_{\max} = 100$, $l_r = 0$). The results of these studies demonstrate the scaling behavior $\ell/M = f(D/M)$ (see Fig. 5). We attribute the remaining difference between the two models to a smaller sample size for the billiard (100 vs 600) and finite $l_r \sim l_{\max}$ values there. For $D \gg M$ the scaling reproduces the estimate (4) while for $D < M$ the length ℓ remains close to M. In this case, the evolution operator becomes a band random matrix of width M with strong *diagonal* fluctuations. They are much larger than the off-diagonal matrix elements so that $\ell \sim M$ for $1 < D < M$ [18].

Let us now discuss how the above properties of eigenstates will affect the characteristics of resonators with rough boundaries. In optical resonators the rays with large reflection angle escape from the system [9]. Because of that there is an effective absorption in the momentum space for $l < l_c$ where l_c is determined by the reflection index so that typically $l_c/l_{\max} \approx 1/2$. This absorption affects the Q value of the resonator which is approximately equal to the number of collisions until the escape. In the ergodic regime this number is determined by diffusive spreading

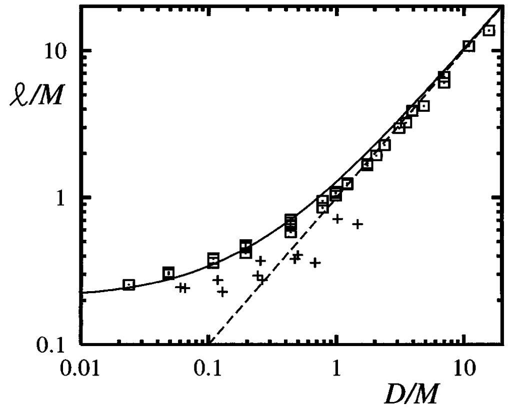

FIG. 5. Rescaled localization length ℓ/M as a function of rescaled diffusion rate D/M for $l_{\max} = 100$: crosses are numerical data for billiards with $0.008 < \tilde{\kappa} < 0.027$ and $20 \leq M \leq 60$; squares are data for the effective kicked rotator model (see text) with $0.006 < \tilde{\kappa} < 0.043$, $5 \leq M \leq 60$, and a matrix size of 600; the full curve is the fit $\ell = 0.5M/\ln[1 + 0.5/(0.05 + D/M)]$ with the asymptotic limit $\ell = D$ shown by the dashed line.

in the momentum space so that $Q \sim l_c^2/D \sim \tilde{\kappa}^{-2}$ being proportional to the inverse Thouless energy. On the other hand, in the localized regime the probability to reach l_c is exponentially suppressed. The subsequent estimate gives $\ln Q \sim l_c/\ell \sim 1/(l_{\max}\tilde{\kappa}^2) > 1$ and for given $l_{\max}$ determines the roughness border $\tilde{\kappa}_Q \approx 1/(2\sqrt{l_{\max}})$ in the Q spoiling which corresponds to our ergodic border (5).

Above we discussed the effects of the rough boundary in a circular billiard. However, we can argue that similar effects should be observed in more general types of convex smooth billiards. Indeed, in such systems, a large fraction of the phase space is integrable and characterized by two action variables (quantum numbers). As in the circular case the rough boundary will lead to a diffusive behavior in one of the actions parallel to the energy surface, and again the quantum interference effects can give its localization. We note that our results are valid for weakly rough billiards $\kappa \ll 1$ while the case of strong roughness $\kappa \sim 1$ deserves separate studies.

A generalization to the three dimensional (3D) case represents an interesting direction for further research. We expect that for a sphere with rough boundary the above 2D analysis is very relevant. Indeed, in a perfect sphere a trajectory is confined to a plane and the precession frequency of this plane is zero. Because of roughness this plane will slowly precess with a frequency proportional to κ. This adiabatic process will weakly affect the dynamics and quantum localization inside the plane section. The localization should give rise to the Shnirelman peak in 3D. However, the situation should be quite different in more general 3D smooth integrable billiards (e.g., ellipsoid). There the precession frequency is rather high due to asymmetry of the smooth boundary, and the diffusion becomes really two dimensional on the energy surface. As for localization in 2D disordered systems, one might expect an exponential fast increase of ℓ with the roughness ($\ln \ell \sim l_{\max}^2 \kappa^2$).

We wonder if the periodic orbit approach can lead to a deeper understanding of spectral properties when quantum effects break classical ergodicity on an energy surface with diffusion.

*Also at Budker Institute of Nuclear Physics, 630090 Novosibirsk, Russia.

[1] O. Bohigas, M.-J. Giannoni, and C. Schmit, Phys. Rev. Lett. **52**, 1 (1984); O. Bohigas, in Ref. [3].
[2] M. L. Mehta, *Random Matrices* (Academic Press, New York, 1991).
[3] *Chaos and Quantum Physics,* Les Houches Lecture Series 52, edited by M.-J. Giannoni, A. Voros, and J. Zinn-Justin (North-Holland, Amsterdam, 1991).
[4] G. Casati, B. V. Chirikov, J. Ford, and F. M. Izrailev, in *Stochastic Behavior in Classical and Quantum Hamiltonian Systems,* Lecture Notes in Physics Vol. 93 (Springer, Berlin, 1979), p. 334; B. V. Chirikov, in Ref. [3].
[5] F. Borgonovi, G. Casati, and B. Li, Phys. Rev. Lett. **77**, 4744 (1996).
[6] Ergodicity is understood in the sense of Shnirelman [11(b)].
[7] S.-X. Qian, J. Snow, H.-M. Tzeng, and R. K. Chang, Science **231**, 486 (1986).
[8] Y. Yamamoto and R. E. Slusher, Phys. Today **46**, No. 6, 66 (1993).
[9] A. Mekis, J. U. Nöckel, G. Chen, A. D. Stone, and R. K. Chang, Phys. Rev. Lett. **75**, 2682 (1995).
[10] V. M. Akulin, C. Bréchignac, and A. Sarfati, Phys. Rev. Lett. **75**, 220 (1995).
[11] A. I. Shnirelman, Usp. Mat. Nauk. (a) **30**, N4, 265 (1975); (b) **29**, N6, 18 (1974).
[12] B. V. Chirikov and D. L. Shepelyansky, Phys. Rev. Lett. **74**, 518 (1995).
[13] B. V. Chirikov, Phys. Rep. **52**, 263 (1979).
[14] K. M. Frahm and D. L. Shepelyansky (to be published).
[15] D. L. Shepelyansky, Phys. Rev. Lett. **56**, 677 (1986).
[16] R. Blümel and U. Smilansky, Phys. Rev. Lett. **69**, 217 (1992).
[17] This time reversal symmetry does not contradict to the value $\beta = 2$ corresponding to the *local* unitary case.
[18] Such a superimposed BRM situation was studied in D. L. Shepelyansky, Phys. Rev. Lett. **73**, 2607 (1994). Similarly, the billiard eigenfunctions should have in $\tan \mu_l$ the Breit-Wigner width $\Gamma_\mu \sim D/M^2$ and $\ell = D$ for $M < D < M^2$ if all γ_m have the same typical value (in energy $\Gamma_E \approx \hbar^2 l_{\max}\Gamma_\mu/mR_0^2$) [14].